

# Research Note: Automated data-driven alignment of near-bit and top-drive vibration sensors for seismic while drilling and beyond

Anton Egorov<sup>1\*</sup>, Ilya Silvestrov<sup>2</sup>, Andrey Bakulin<sup>2</sup> and Pavel Golikov<sup>1</sup>

<sup>1</sup>Aramco Research Center Moscow, Aramco Innovations LLC, Leninskiye Gory 1-75B, Moscow, 119234, Russia, and <sup>2</sup>EXPEC Advanced Research Center, Saudi Aramco, Dhahran, Saudi Arabia

Received February 2021, revision accepted May 2021

## ABSTRACT

Downhole near-bit vibration sensors are used to record the pilot signal for seismic while drilling and identify drilling dysfunctions for drilling optimization. The typical downhole sensor is a memory-based device with an inexpensive internal clock of limited accuracy that is not synchronized to surface data. Integrating downhole vibrations with other time-based data such as surface drilling parameters or seismic recordings requires accurate time alignment between all data sets. We present a novel automated two-step alignment procedure that uses a Global Positioning System-synchronized top-drive vibration sensor as a reference. The accuracy of the new method satisfies the most demanding requirements of seismic while drilling. The first step finds the delay time and linear drift using global optimization. The second step estimates nonlinear drift using time-variant cross-correlation. Alignment precision of a few seconds after the first step becomes a few milliseconds after the second step, as demanded by seismic-while-drilling. The field data example shows that the proposed methodology successfully aligns top-drive and downhole data using a fully unsynchronized near-bit vibration data set. After alignment, the near-bit sensor delivers a usable pilot for seismic-while-drilling processing, resulting in better quality correlated seismic data than those obtained with the top-drive surface pilot.

**Key words:** Borehole geophysics, Data processing, Seismic while drilling.

## INTRODUCTION

Seismic waves emitted by a drill bit during drilling are recorded in seismic-while-drilling (SWD) acquisition by surface sensors installed around the rig or by downhole sensors deployed in a nearby well (Poletto and Miranda, 2004). Additional vibration sensors are often used to obtain the drill-bit signature or a so-called pilot required for correlation with surface geophones similar to vibroseis technology. These sensors can be placed near the top of the drillstring (usually mounted on the top drive) or downhole near the bit. Since the downhole sensor is closer to the bit, it often provides less contaminated and more accurate drill-bit signal representation. Apart

from SWD, vibrations recorded by the near-bit sensor can be used for other applications, such as drilling dynamics analysis (Jones and Sugiura, 2020), identification of boundaries between the formations (Myers *et al.*, 2002) or direct prediction of formation properties (Glubokovskikh *et al.*, 2020). Reliable processing and interpretation of the drillstring vibration data require synchronization with other logging and recording systems installed on the rig. The accuracy of this synchronization depends on the particular application. It can vary from several seconds for drilling dynamics analysis to milliseconds for SWD. The top-drive data are usually readily available in real time and can be easily synchronized to a GPS clock. Real-time recording and synchronization of the near-bit vibration data are more challenging to achieve. There are high-end ultrahigh-precision downhole clocks for costly offshore wells with a very

---

\*Email: anton.egorov@aramcoinnovations.com

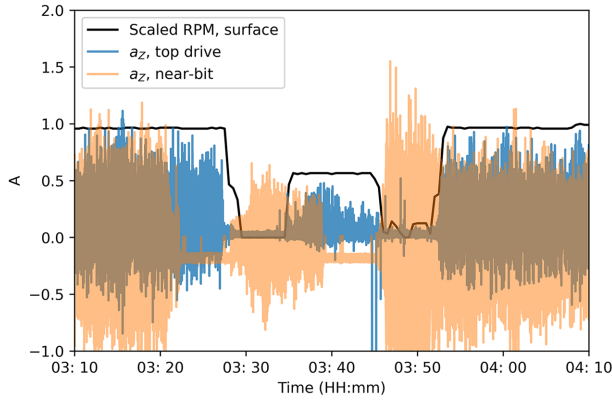


**Figure 1** A comparison of drilling RPM recorded at the surface (black) with the top-drive (blue) and near-bit (orange) accelerations. RPM and top-drive sensors appear synchronized. High RPM values coincide with intense surface vibrations. In contrast, the near-bit acceleration is shifted significantly.

small drift of 1 ms per 10 days (Vieitez and Cox, 2017). Most vibration tools used in onshore drilling utilize inexpensive unsynchronized clocks that have a significantly higher drift. Data from such memory-based sensors are extracted when the bottomhole assembly is pulled out and brought to the surface after a typically multi-day drilling run. As a result, the clock errors tend to be large and require a significant correction. Fast telemetry, such as wired drill pipe technology (Naville *et al.*, 2004; Poletto *et al.*, 2014), may offer real-time data transmission and an alternative solution to solve the time-alignment issue using existing tools; however, it has received limited penetration in the industry thus far. This study aims to solve this problem for conventional memory-based near-bit sensors with inexpensive unsynchronized clocks experiencing significant and temperature-dependent drift. We solve the problem using a data-driven approach that directly correlates downhole vibrations to the reference top-drive surface sensor with a GPS-synchronized clock.

We demonstrate the new approach using the field data set collected during a recent first onshore trial of the Drill-CAM system (Bakulin *et al.*, 2019) with an unsynchronized and drifting near-bit vibration sensor. The clock drift was relatively high, with the clock error at the end of a drilling run (60–120 hours) reaching 30–40 minutes. An example of a raw uncorrected data fragment can be seen in Figure 1, where the discrepancy in the timing of near-bit and top-drive sensors is apparent. To overcome this issue, we suggest a two-step procedure to estimate the misalignment and correct the clock from the near-bit vibration sensor by aligning it with the top-drive vibration recordings. The first step is a novel optimization-

based procedure for estimating the clock drift's linear component and the constant time delay. The second step is a time-variant cross-correlation (TVCC) analysis of top-drive and near-bit sensors similar to the one discussed by Naville *et al.* (2004). The processing result of the first step has an accuracy of a few seconds, so it is acceptable to analyse drilling dysfunctions for drilling optimization. The second step (applicable only when a few seconds accuracy is reached) is needed to reduce the error to a few milliseconds as required for SWD applications.

In addition to cross-correlations that are readily available from TVCC analysis, we compare the top-drive and near-bit pilot traces' autocorrelations to validate the result. To validate the achieved accuracy for SWD, we correlate the corrected near-bit vibration recordings with the geophone data recorded in the rig's vicinity while drilling. It provides a conventional reverse VSP gather with a source located in the borehole and a surface line of receivers. Comparing the results with a similar SWD gather obtained using the top-drive sensor confirms that accurate alignment was achieved.

## CLOCK-DRIFT CORRECTION METHOD

### Step 1: A time delay and linear drift (few seconds accuracy)

The proposed time-alignment procedure starts with a global optimization step to estimate the unknown time shift and the drift's linear component. We search for two scalar parameters – shift  $s$  and drift  $d$  – to create a linear mapping between the time for the near-bit acceleration recording and the synchronized top-drive time:

$$t^{td} = (1 + d)t^{nb} + s; \quad t^{nb} = (t^{td} - s)/(1 + d). \quad (1)$$

Here, the quantities  $t^{td}$  and  $t^{nb}$  are the time samples for the top-drive and near-bit sensors. Both series have the same time origin corresponding to when the battery was installed in the near-bit sensor. Values of  $d = 0$  and  $s = 0$  would mean that the near-bit clock is entirely accurate. Here,  $d$  is dimensionless, while  $s$  is expressed in seconds. In the following section, superscripts  $^{td}$  and  $^{nb}$  stand for top-drive and near-bit, respectively.

In a typical drilling case, the drillstring rotation speed in rotations per minute (RPM) is measured at the surface and by another sensor inside the downhole tool. If available, these RPM curves can be used for the first step of clock-drift correction. Being one of the most fundamental drilling measurements, RPM is almost always available. We can form a misfit function based on the difference of RPM curves following

equation (2) and search for optimal values  $\hat{d}$  and  $\hat{s}$  that minimize such misfit. For this minimization procedure, we have used constrained grid search and simplex search algorithms. Both methods delivered similar results. With the appropriate set-up, the simplex search performs minimization faster. The grid search is a robust solution that does not require any parameter setting, so we prefer to use it instead to achieve maximum automation.

$$J(d, s) = \sum_{t^{td}} \left( RPM^{td}(t^{td}) - RPM^{nb} \left( (t^{td} - s) / (1 + d) \right) \right)^2;$$

$$\hat{d}, \hat{s} = \operatorname{argmin} J(d, s). \quad (2)$$

Suppose RPM curves are unavailable (i.e. when one of the RPM sensors fails). In that case, the least-squares misfit of waveform difference in the recorded top-drive and near-bit accelerations can be minimized directly. Here, we use only vertical components of accelerations,  $a_z^{td}(t^{td})$  for the top-drive sensor and  $a_z^{nb}(t^{nb})$  for the near-bit sensor:

$$\sum_{t^{td}} \left( a_z^{td}(t^{td}) - a_z^{nb} \left( (t^{td} - s) / (1 + d) \right) \right)^2 \rightarrow \min. \quad (3)$$

This step requires an interpolation/resampling procedure for the near-bit sensor for each misfit calculation (so that  $a_z^{td}(t^{td})$  and  $a_z^{nb}((t^{td} - s)/(1 + d))$  are on the same discrete-time grid). Consequently, conducting any optimization is computationally costly, given the length of the processed time series is tens of hours and submillisecond sampling. Also, using the waveform misfit can further be hampered by disparate phase characteristics of two sensors. We choose to compute a specific envelope attribute from the initial accelerations on a decimated time grid and use it for optimization to mitigate this. In principle, any attribute that carries the main signal characteristics can be considered. One option is to use the total energy of vibrations (sum of squared amplitudes) in a selected time window,  $E^{td}$  and  $E^{nb}$ , for the top-drive and near-bit sensors. So, we look for  $\hat{d}$  and  $\hat{s}$  that minimize the following misfit:

$$J(d, s) = \sum_{t^{td}} \left( E^{td}(t_{dec}^{td}) - E^{nb} \left( (t_{dec}^{td} - s) / (1 + d) \right) \right)^2;$$

$$\hat{d}, \hat{s} = \operatorname{argmin} J(d, s). \quad (4)$$

Here, subscript ‘dec’ describes a decimated time series with a chosen time window size (30 s in our case, which is also the decimated series’ sampling interval, as we use non-overlapping windows). To minimize the misfit, we use a constrained grid search. From our experience, this misfit has a

single minimum for practically observed values of drift and shift, which will be demonstrated for a field example below.

We have found that the top-drive sensor’s windowed energy attribute is susceptible to high-amplitude noise generated by different operations on the drilling rig. In this case, it is worth applying bandpass/notch filtering before computing the attribute or use noise removal (such as median filtering) after its computation.

Once the optimal  $\hat{d}$  and  $\hat{s}$  are identified, the correction is introduced by converting the near-bit time to GPS-synchronized top-drive time using the linear transformation (1). This results in a data set with the sampling rate  $f_{rec}/(1 + d)$ , where  $f_{rec}$  is the original sampling frequency of the near-bit tool. If such sampling frequency is inconvenient, an additional Fourier resampling step to  $f_{rec}$  can be conducted on transformed time series.

## Step 2: Nonlinear drift (few milliseconds accuracy)

The linear correction step above usually aligns the data with the accuracy of a few seconds, paving the way for the second step refining it to a few milliseconds. This is achieved using the conventional time-variant cross-correlation analysis in time windows with 30 s length. We divide the top-drive and the near-bit sensors’ recordings into time windows and compute their cross-correlations. The lag of the cross-correlation’s maximum identifies the remaining drift that needs to be corrected. This method allows for the correction of nonlinear drift. These residual corrections are often in the order of a few seconds.

The described automatic two-step procedure achieves alignment between the top-drive and near-bit data sets acceptable for seismic-while-drilling applications. It remains to account for the time delay caused by signal propagation along the drillstring between downhole and top-drive sensors. Introducing appropriate corrections into the sensors’ recordings provides the true downhole time (Poletto and Miranda, 2004).

## FIELD DATA EXAMPLE

### Alignment of the top-drive and near-bit sensors

The data used in the following examples were obtained during the onshore field trial presented by Bakulin *et al.* (2019). A real-time three-component accelerometer sensor installed on the top drive was used simultaneously with the memory-based downhole vibration tool down to  $\sim 3,050$  m (10,000 ft) depth. Since the recorded borehole segment is nearly vertical,

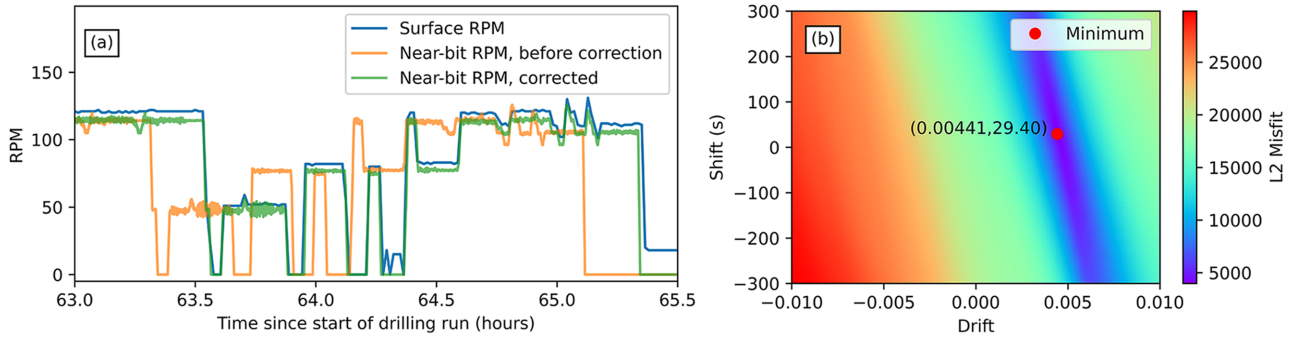


**Figure 2** (a) Surface (blue), uncorrected downhole (orange) and corrected downhole (green) drilling RPM. (b) A misfit function computed for a wide range of values of drift and shift; the minimum of the misfit function found by the optimization is highlighted with a red dot. Used data represent a subset from a single drilling run, 1,275–1,600 m (4,180–5,246 ft). Identified optimal values are  $d = 0.00441$  and  $s = 29.40$  s.

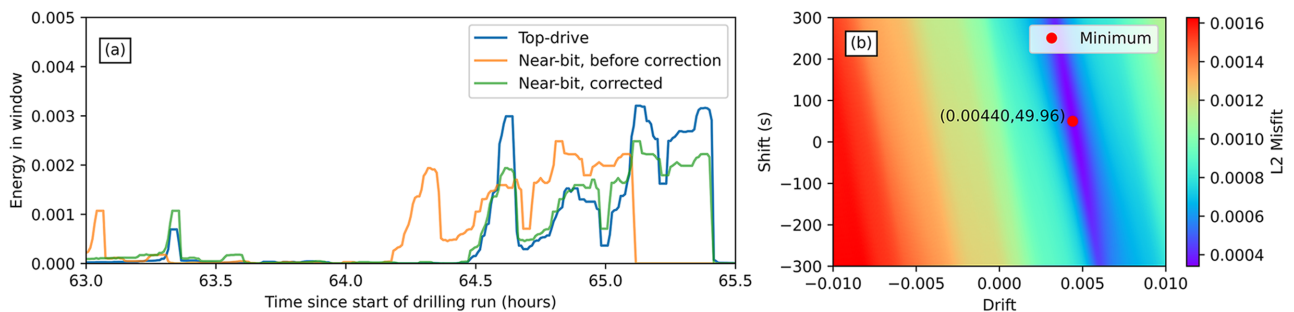


**Figure 3** (a) Energy attribute computed in 30 s time windows using vertical acceleration from the top-drive sensor (blue), uncorrected near-bit sensor (orange) and corrected near-bit sensor (green). (b) A misfit function computed for a wide range of values of drift and shift; the minimum of the misfit function is highlighted with a red dot. The same subset of the data as in Figure 2 from a single drilling run, 1,275–1,600 m (4,180–5,246 ft). Identified optimal values are  $d = 0.00440$  and  $s = 49.96$  s.

only the Z acceleration component is used in this study. In addition to accelerometers, the downhole tool contains gyro sensors that estimate downhole RPM near the bit. A typical example of clock drift can be observed on the drilling RPM curves recorded on the surface (blue) and downhole (orange), as shown in Figure 2(a). Traditional clock-drift correction workflow for such a near-bit tool would involve manual picking of the same events on the two curves and using those picks for calculation of drift  $\hat{d}$  and shift  $\hat{s}$ . The presented methodology eliminates all manual steps and replaces them with fully automatic computation of  $\hat{d}$  and  $\hat{s}$  using misfit minimization. The misfit is shown in Figure 2(b), and the corrected downhole RPM is displayed as a green line in Figure 2(a).

Figure 3(a) shows an example of drift estimation directly from the top-drive and near-bit accelerations. It compares a segment of top-drive energy (blue line) to near-bit energy before (orange line) and after time alignment (green line) with obtained  $\hat{d}$  and  $\hat{s}$ . We compute  $E^{td}$  and  $E^{nb}$  in the seismic frequency band after filtering the accelerations by a suitable bandpass filter (Ormsby bandpass with 15–25–40–80 Hz for

the examples below). A small 7-point median filter was applied to the energies to remove outliers. The timing inconsistency between the top-drive and uncorrected near-bit energies can be identified and is eliminated by the correction. Figure 3(b) shows the misfit for the used range of values of  $d$  and  $s$  ( $\pm 0.01$  for  $d$  and  $\pm 5$  minutes for  $s$ ). There is only one minimum that can be clearly identified. Note that the drift and shift estimation in Figures 2 and 3 was conducted for the same drilling run; however, the estimated values are quite different. There are a few causes for such differences. First, the records used for alignment are relatively coarsely sampled. The RPM curves have 5 s sampling (the original downhole RPM is much more finely sampled; however, the surface RPM is sparse). The sample interval of the selected energy attribute is 30 s. Second, while there is only one global minimum, the misfit function has a pronounced elongated valley (Figure 3b). It means that certain pairs of shift and drift along this valley lead to virtually identical misfit values. Such a valley explains why we obtain different shift values in Figures 2 and 3 using the same drilling run data. Both optimal values reside along this valley and lead



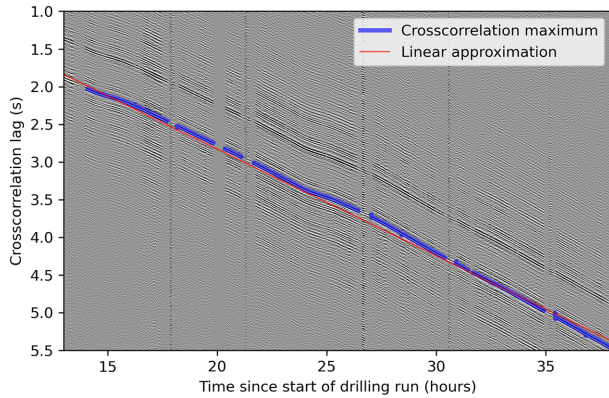


**Figure 4** Cross-correlation of the top-drive and near-bit acceleration recordings after the automatic linear timing correction (first stage of our alignment workflow). Picked cross-correlation maxima are displayed in blue; the remaining linear drift component is displayed in red. Blank spaces correspond to the quiet intervals without drilling.

to a similar misfit, thus providing equally suitable alignment. Indeed, Figures 2(a) and 3(a) show that both estimates align the time series at hand, which is the main task of the algorithm. The certain trade-off between the shift and drift does not impact the ultimate goal of obtaining an accurate down-hole pilot, and any residual errors left would be corrected in the next nonlinear correction step.

It is important to note that the linear correction of drift is fully automatic and data-driven. Many factors limit the accuracy of the linear timing correction. It often allows bringing the timing error from tens of minutes to a few seconds. After this, the cross-correlation-based timing correction can be applied to remove the remaining smaller errors. Examples of cross-correlations between the top-drive and near-bit accelerations after the linear timing correction computed in 30-s-long time windows are shown in Figure 4. It can be seen that a small fraction of drift's linear component remains in the data, but it is now reduced to a few seconds over the displayed 25 hours of acquisition. This remaining linear drift can be used to update the estimates of  $\hat{d}$  and  $\hat{s}$  obtained on the previous stage by fitting a straight line through the picked cross-correlation maxima. Of course, the picks can be directly used to remove clock drift. However, we first intend to understand the magnitude of nonlinear timing error. After extracting this remaining linear component and selecting only those traces that correspond to active drilling, the error due to purely nonlinear drift in Figure 5(a) becomes lower than 0.25 s. With these picks, the residual drift can be corrected. After the correction, cross-correlations are displayed in Figure 5(b), where the maxima are aligned at zero lag. The second high-amplitude event, which has a staircase-like shape,

corresponds to the cross-correlation between the direct wave propagating in the drillstring and the first-order multiple. The delay of this multiple is constant for a fixed drillstring length. It changes discretely when the new drill pipes are added to the drillstring. The two-way analytical time in the drillstring was computed for this drilling segment using the drillstring propagation velocity of 4,960 m/s. It is displayed as a red line in Figure 5(b) and aligns well with the described event.

Several factors control the quality of the correlation between top-drive and near-bit sensors. Depth of the bit would determine propagation distance and hence signal attenuation. The size and type of the bit would influence the strength of the excited signal. Surface noise on the top-drive (not associated with the drill bit) may reduce the correlation. It is instructive to analyse how this correlation quality depends on the depth and main factors above. Figure 6 shows the maximum value of normalized cross-correlation between the top-drive and near-bit accelerations versus depth (this was computed after filtering the accelerations with 15–25–40–80 Hz Ormsby bandpass filter). This value can be considered as a correlation coefficient (or correlation quality) after the corresponding time correction is applied to the downhole data. Both roller-cone (RC) and polycrystalline diamond compact (PDC) bits were used for drilling in this data set; the size and type of the bits are also shown. Figure 6 provides an insight into how reliable the correlation-based time alignment is. We observe that the best correlation occurs between 820 m (2,700 ft) and 1,890 m (6,200 ft) with a maximum value of approximately 0.6. In the deeper part, the maximum cross-correlation amplitude quickly drops to 0.1, likely because of the smaller PDC bit exciting less axial energy that further suffers from larger attenuation due to longer propagation path. Above 820 m (2,700 ft), the cross-correlation is also relatively small and is slightly higher than 0.1, perhaps because of additional surface noise contaminating the top-drive signal. This specific onshore well suggests that the drilling interval at the medium depth of 820–1,890 m (2,700–6,200 ft) may be the most reliable in terms of time alignment. Despite lower correlation in the shallow and the deep intervals, estimated time corrections remain usable at least for shallow intervals, as confirmed by further comparisons of the seismic-while-drilling (SWD) gathers (not shown here). In general, we observed higher values of cross-correlation for RC bits.

### Analysis of autocorrelations

Autocorrelations of the recorded drillstring signal are typically used to evaluate the pilot's quality for SWD (Poletto

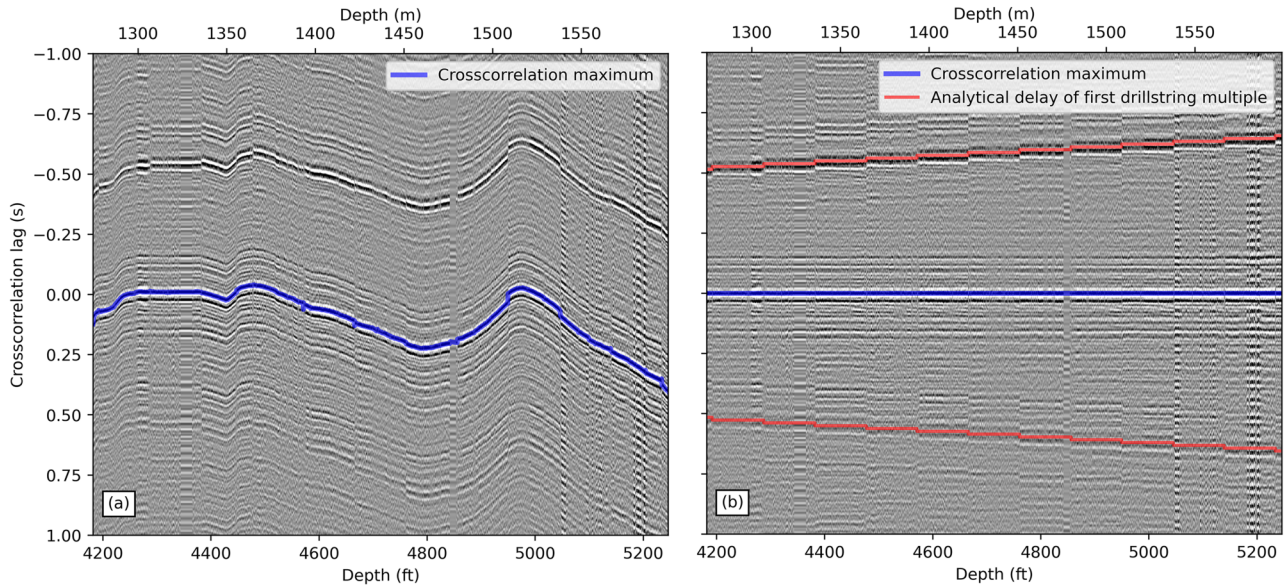


**Figure 5** Cross-correlation of the top-drive and near-bit acceleration recordings before (a) and after (b) removal of nonlinear drift using TVCC correction. Analytically computed delays of the first drillstring multiple are overlaid on the cross-correlation plot in (b).

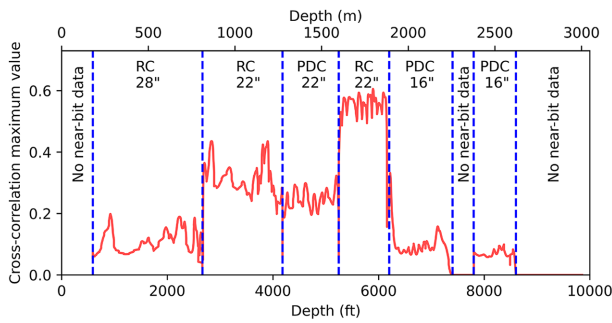


**Figure 6** Maximum values of cross-correlation between top-drive and near-bit accelerations plotted versus depth. Bit types are labelled RC for a roller-cone and PDC for a polycrystalline diamond compact bit, bit diameters are provided in inches. Observe low values of cross-correlation in the deepest portion of the well drilled with PDC and the shallowest section with RC.

and Miranda, 2004). Drillstring multiples observed on the autocorrelations allow estimating the drillstring propagation velocity and judging the recordings' overall signal-to-noise ratio. Figure 7 shows the examples of the autocorrelations for the top-drive and near-bit pilots' recordings computed for 30 s time windows. The near-bit pilot has already been aligned with the top-drive using the proposed method. Coherent events away from zero lag indicate the presence of recorded multiple reflections in the drillstring. Non-drilling intervals can be easily identified as ensembles of records with low en-

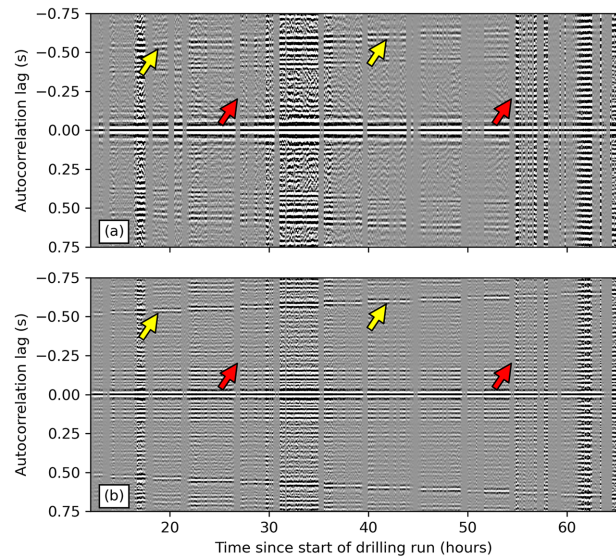


**Figure 7** Autocorrelations of the top-drive (a) and near-bit acceleration recordings after time alignment (b). Low-energy zones marked by red arrows correspond to non-drilling intervals. Observe excellent alignment of non-drilling and drilling intervals between the two data sets. Strong horizontal events away from zero time lag correspond to drillstring multiples (yellow arrows) that occurred while drilling.

ergy. We note a good correspondence between the drilling and non-drilling intervals in both pilots, supporting a perfect alignment of the downhole data using the proposed algorithm. The downhole pilot tends to provide a better signal-to-noise ratio

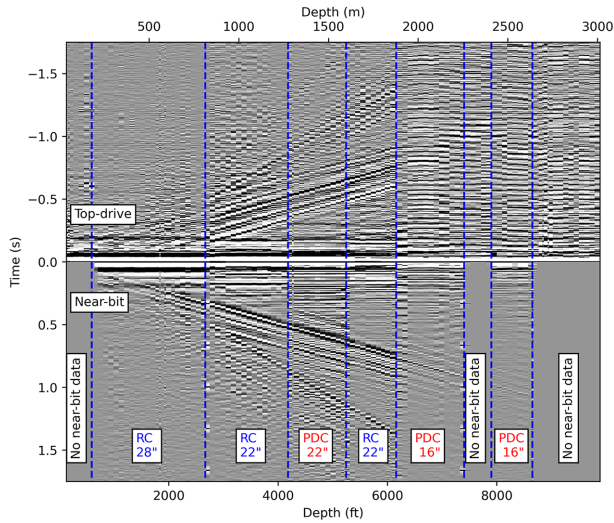


**Figure 8** A comparison of deconvolved autocorrelations for top-drive (top) and near-bit (bottom) sensors. The drilling intervals with RC and PDC bits are labelled. The empty intervals in the near-bit sensor autocorrelations mark the intervals with no recordings due to the battery failure.

manifesting itself in less noisy non-drilling intervals and more coherent drillstring multiples. The deconvolved and stacked (over a drilling interval equal to one drill pipe stand) autocorrelations for all the recorded depths are shown in Figure 8. Again, we observe a good match between both data sets and reasonable behaviour of the downhole pilot autocorrelations after the time alignment. The drillstring multiples have relatively strong amplitude until 1,890 m (6,200 ft). Deeper PDC bits had a lower diameter, which influences the signal level. The multiples are entirely masked by noise in top-drive data below this depth. In downhole data, they have low energy, but still can be partially identified. It suggests that the downhole sensor may allow capturing of a weaker drill-bit signal even in the PDC-drilled section below 1,890 m (6,200 ft).

### Analysis of seismic gathers

After applying the proposed method, the top-drive and the near-bit sensors are aligned in time. However, the alignment procedure implicitly assumes that these sensors are co-located, which does not reflect reality. The downhole tool records signal near the source, whereas the top-drive sensor records the same signal at the other end of the drillstring near the surface. Therefore, to obtain true downhole time, near-bit data should be moved back in time by the drillstring wave propagation time between bit and top drive. To use top-drive data as a

pilot, it should also be moved with the same drillstring propagation time (Poletto and Miranda, 2004), estimated from the multiples in Figure 7.

After this correction, both pilots properly characterize drill-bit source function in GPS time. Then correlation of the pilot signals with the geophone data recorded at the surface is performed to convert the continuously recorded seismic data to conventional impulse-source seismograms. This is followed by accumulating and stacking of the correlated signal over some time or depth interval to improve the signal-to-noise ratio. A one-sided pilot deconvolution is finally applied (Poletto and Miranda, 2004) to attenuate the anti-causal reverberations in the seismic gather caused by the drillstring multiples. Figure 9 shows an example of the obtained common-shot (or common-bit) seismograms using top-drive and near-bit pilots for the drill bit at 1,160 m (3,810 ft) depth. Kinematically, the top-drive and near-bit results are similar. However, the near-bit pilot sensor provides an improved signal-to-noise ratio with more clearly visible first arrivals. These results illustrate that the proposed time-alignment scheme allows correcting the clock errors in the memory-based near-bit vibration sensors to the accuracy required by seismic-while-drilling applications.

## DISCUSSION

It is important to note that this work is devoted to enabling the usage of conventional off-the-shelf memory-based downhole vibration tools with unsynchronized drifting clocks for advanced applications such as seismic-while-drilling without introducing any hardware modifications. If the downhole clock is accurate enough (Vieitez and Cox, 2017), such corrections are not required. This is rarely the case for most downhole near-bit vibration tools currently adopted in the industry. Presented work demonstrates that even with an inaccurate and fully unsynchronized clock, seismic-while-drilling (SWD) processing with the near-bit pilot sensor is possible down to a certain depth when correlated signal reliably registers on the top-drive reference sensor. Our proposed method's first step allows for a fully automatic correction of time shift and linear drift resulting in a few seconds' timing accuracies. If the vibration data are used for other purposes than SWD, such as drilling dynamics analysis or formation identification, then this automatic correction can be enough. The second step requires the picking of cross-correlation maxima. While it can be automated to some extent by autopicking algorithms, we have experienced a need for manual quality control and editing of the picks. If the signal-to-noise ratio of the top-drive



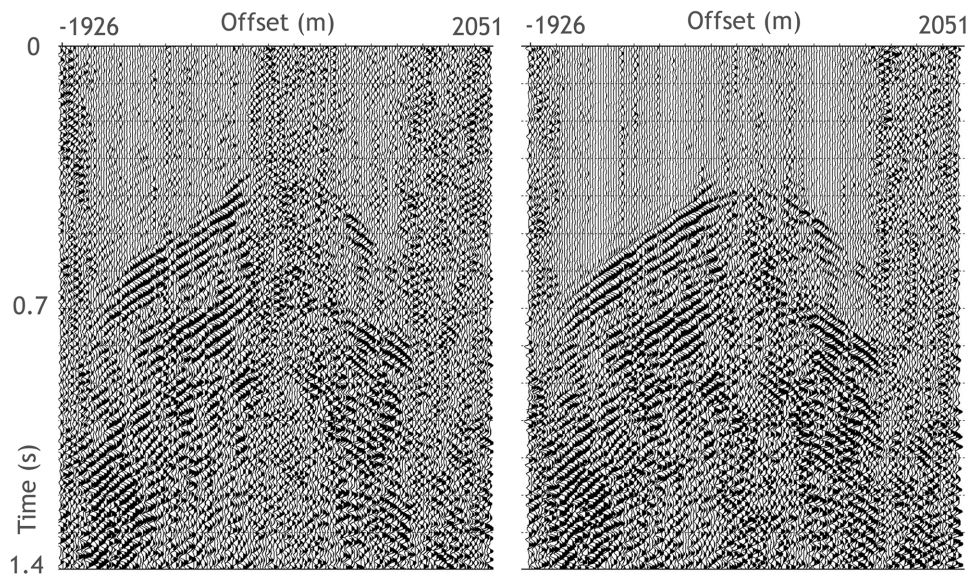


**Figure 9** Seismic gathers computed with top-drive (left) and near-bit (right) pilots after the alignment procedure. Roller-cone bit depth is 1,160 m (3,810 ft).

sensor becomes too low due to strong signal attenuation in the drillstring or excessive surface noise, then such a correction becomes impossible, even if the near-bit sensor continues to record perfectly valid data.

## CONCLUSION

Memory-based near-bit sensors provide a cost-effective solution to record valuable vibration data for seismic-while-drilling and drilling optimization. Their internal clock is typically unsynchronized. Besides, it is susceptible to significant drift over drilling run time, making its application to the processing of seismic-while-drilling data impossible without a correction. We propose a method to address this challenge by data-driven time alignment of near-bit sensor data with surface recordings by Global Positioning System-synchronized top-drive sensor. The first step of the alignment procedure estimates the time shift and the linear component of the clock's drift using global optimization with a few seconds' accuracies. The second step compensates residual nonlinear drift using time-variant cross-correlation analysis with few milliseconds' accuracies acceptable for seismic-while-drilling applications. After precise data-driven time alignment, seismic gathers and pilot autocorrelations are analysed. The seismic gathers computed using the top-drive and near-bit pilot sensors show similar arrivals, confirming that an accurate pilot was obtained from downhole data. Since the procedure is data-driven, the quality of alignment is susceptible to other noises

present in the data and signal attenuation when propagating through the long drillstring. The maximum cross-correlation coefficient is achieved for a depth interval of 820–1,890 m (2,700–6,200 ft). At shallow depth below 820 m (2,700 ft), cross-correlation is reduced, likely due to contamination by intense surface noises. At a depth below 1,890 m (6,200 ft), cross-correlation is also reduced, possibly because of usage of polycrystalline diamond compact bits generating weaker signals that further suffer from more significant attenuation due to long propagation distances from the bit to the top drive. Consistent with this observation, the near-bit data autocorrelations reveal lower amplitudes of the multiples recorded for deeper drilling runs (traversing the drillstring twice). Similar multiples cannot be observed on top-drive data autocorrelations (traversing the drillstring three times). The seismic gathers' resulting quality is higher for the near-bit pilot, suggesting that the use of the downhole vibration signature for seismic-while-drilling applications is promising. An in-depth analysis and comparison of the time-aligned top-drive and near-bit recordings in the considered field study is a topic of ongoing research.

## ACKNOWLEDGEMENTS


We thank Flavio Poletto (OGS) for sharing his experience and advice during the study. We are thankful to Grant Corrie and Sahet Keshiyev (both of NOV) for a fruitful discussion on existing alignment approaches for drilling optimization


applications. We are grateful to Yue Du and Yujin Liu (both of the Aramco Research Center Beijing) for their initial assessment of the synchronization issue in the considered field study. This paper also benefited from the constructive suggestions from Mustafa Al-Ali, Timur Zharnikov (both of the Aramco Research Center Moscow), Emad Hemyari, and Robert Smith (both of Saudi Aramco).


#### DATA AVAILABILITY STATEMENT


The data studied in this paper are confidential and are not shared.

#### ORCID

Anton Egorov  <https://orcid.org/0000-0001-9139-6191>

Ilya Silvestrov  <https://orcid.org/0000-0002-2394-3576>

Andrey Bakulin  <https://orcid.org/0000-0002-6638-7821>

Pavel Golikov  <https://orcid.org/0000-0002-9223-1273>

#### REFERENCES

- Bakulin, A., Hemyari, E. and Silvestrov, I. (2019) Acquisition trial of DrillCAM: Real-time seismic with wireless geophones, instrumented top drive and near-bit accelerometer. 89th Annual International Meeting, SEG, Expanded Abstracts, 157–161. <https://doi.org/10.1190/segam2019-3214516.1>
- Glubokovskikh, S., Bakulin, A., Smith, R. and Silvestrov, I. (2020) Machine learning algorithms for real-time prediction of the sonic logs based on drilling parameters and downhole accelerometers. 90th Annual International Meeting, SEG, Expanded Abstracts, 405–409. <https://doi.org/10.1190/segam2020-3427085.1>
- Jones, S. and Sugiura, J. (2020) Analysis of surface and downhole drilling dynamics high-frequency measurements enhances the prediction of downhole drilling dysfunctions and improves drilling efficiency. Abu Dhabi International Petroleum Exhibition & Conference, SPE-202859-MS. <https://doi.org/10.2118/202859-MS>
- Myers, G., Goldberg, D. and Rector, J. (2002) Drill string vibration: a proxy for identifying lithologic boundaries while drilling. In: Casey, J.F. and Miller, D.J. (eds) *Proceedings of the Ocean Drilling Program, Scientific Results*, Vol. 179. Ocean Drilling Program, pp. 1–17.
- Naville, C., Serbutoviez, S., Throo, A., Vincké, O. and Cecconi, F. (2004) Seismic while drilling (SWD) techniques with downhole measurements, introduced by IFP and its partners in 1990–2000. *Oil & Gas Science and Technology*, 59(4), 371–403. <https://doi.org/10.2516/ogst:2004027>
- Poletto, F. and Miranda, F. (2004) *Seismic While Drilling: Fundamentals of Drill-Bit Seismic for Exploration*. Elsevier.
- Poletto, F., Miranda, F., Corubolo, P., Schleifer, A. and Comelli, P. (2014) Drill-bit seismic monitoring while drilling by downhole wired-pipe telemetry. *Geophysical Prospecting*, 62, 702–718. <https://doi.org/10.1111/1365-2478.12135>
- Vieitez, C. and Cox, M. (2017) Walkaway seismic-while-drilling operation delineates salt dome. *Offshore*, 77(7). <https://www.offshore-mag.com/production/article/16755923/walkaway-seismicwhiledrilling-operation-delineates-salt-dome>